

# Characterization of a Capacitive Position Sensor for a Miniaturized Hydraulic Actuator

Laura M. Comella, Krasimir Ayvazov, Timo Cuntz, Auguste van Poelgeest, Jonathan Schächtele, and Jan Stallkamp

**Abstract**—Novel surgical techniques require laparoscopic instruments which are intelligent micro-manipulators rather than simple manually operated scissors. Hydraulic drives, with their high force and power density, and low weight are the perfect candidates to drive these new laparoscopic instruments. However, their use in intelligent systems requires the integration of a displacement measurement technology to ensure controllability. The aim of this paper is the characterization and miniaturization of a capacitive sensor that can be integrated into the hydraulic drives in order to improve the precision of the instrument's positioning. The proposed sensor solution is structurally integrated into the hydraulic drive, using its barrel and rod as a coaxial cylindrical capacitor, so that no additional sensor needs to be integrated. The performance of the proposed solution has been examined using FEA simulations of a mini and a miniaturized cylinder design. The simulation has been validated experimentally and the results are in good agreement. The results showed a linear relationship between capacitance and displacement with a precision of  $\pm 27 \mu\text{m}$ , thus proving the feasibility of the method.

**Index Terms**—Actuators, capacitive sensing, displacement measurement, electro-hydraulics.

## I. INTRODUCTION

MINIMALLY invasive surgical procedures are becoming more common due to the advantages that they provide to the patient: short recovery time, and reduced pain and hemorrhage [1]–[3]. However, their complexity is a challenge for the surgeon. Manually driven, mechanical instruments lack freedom in movement, are restricted in their applicable force, and operating their degrees of freedom is cumbersome and requires training.

To meet the requirements of new surgical techniques, various efforts have been made in recent years to develop micro-manipulator systems [4]–[6], which, with the help of control techniques and telemanipulation, facilitate laparoscopic procedures. However, they are not widespread, as the integrated drives make them too heavy to hold or manipulate.

It has been proven that hydraulic drives are characterized by greater force and power density compared to classic mechanical transmissions [7], [8] thus hydraulically driven laparoscopic instruments offer a significantly improved

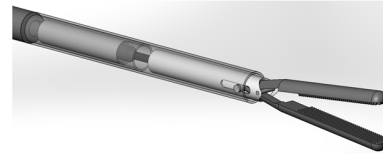


Fig. 1. Design of the laparoscopic instrument tip considered in this article, driven by a hydraulic cylinder with a diameter of 2.5 mm. The cyan and blue components highlight the space available for both the drive and the sensor.

performance over the standard minimally invasive surgical instruments [9]–[12]. Moreover, they are lightweight, because the power generator, the pump, does not have to be placed inside the instrument. All these advantages make hydraulic drives a viable solution for a micro-manipulator system. However, they are not as mechanically rigid compared to instruments with mechanical drive mechanisms due to trapped air, leakage, the compressibility of the medium, and the elasticity of the tubes in hydraulic circuits. Their use in intelligent systems thus requires the integration of a displacement measurement technology. Hence, this research paper investigates sensor methods for the hydraulic drives developed in [13].

Laparoscopic instruments are at the limit of what is technologically feasible in terms of miniaturization: integrating any additional component is a significant challenge. Given the instrument's size, it is not possible to incorporate an off-the-shelf sensor [14], [15], as displacement sensors on the market are designed for large scale cylinders. Even the smallest commercially available displacement sensor would not fit in the limited space at the tip of the instrument, which is already occupied by the hydraulic drive and transmission mechanism, as can be seen in Fig. 1.

Position sensors integrated into micro hydraulic actuators have been presented by Zhu and Book in [16], by Volder, Coosemans, and Reynaerts in [17], and by Sumali, Bystrom and Krutz in [18]. In [16], a capacitively coupled resistive sensor has been developed, whereas in [17] and [18] a miniaturized inductive sensor was presented. All these solutions required the integration of additional elements in the hydraulic cylinder.

The goal of this work is to determine a sensing method which requires as little additional space in the instrument as possible and necessitating the least changes to the existing mechanical design. A capacitive measurement principle [19] is investigated, as the integral structures of the hydraulic cylinder already can be used for such a sensor, without the need of additional elements. This method has been established in

Manuscript received June 17, 2016; accepted October 9, 2016. Date of publication October 26, 2016; date of current version December 8, 2016. The associate editor coordinating the review of this paper and approving it for publication was Prof. Massood Z. Atashbar.

The authors are with the Fraunhofer-Institut für Produktionstechnik und Automatisierung, Mannheim 70569, Germany (e-mail: laura.maria.comella@ipa.fraunhofer.de; yvazov.krasimir@ipa.fraunhofer.de; timo.cuntz@ipa.fraunhofer.de; Auguste.van.Poelgeest@ipa.fraunhofer.de; Jonathan.Schachtele@ipa.fraunhofer.de; Jan.Stallkamp@ipa.fraunhofer.de).

Digital Object Identifier 10.1109/JSEN.2016.2620722

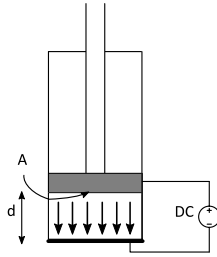


Fig. 2. Schematic of parallel capacitance sensor configuration. The sensor electrodes are: the barrel's base and the top head surface of the piston, in black and grey respectively.

large-scale industrial applications [20], but no investigation of its feasibility on a smaller scale is present in the literature. Hence the objective of this research is to study the scalability of this sensor principle. The following sections present the results of the analytic considerations, the FEA simulations, and the experimental investigation. The simulation and experimental measurements are then compared and discussed. This includes the discussion on the influence of mechanical tolerances on the measurements.

## II. THE CAPACITIVE POSITION SENSOR

### A. Principles of Operation and Theoretical Investigation

Capacitive sensors typically consist of parallel electrode plates and a dielectric. The capacitance  $C$  is an electrical property of the capacitor and designates the amount of charge that can be stored on its electrodes in relation to the applied voltage. This value depends on the geometry of the capacitor and the characteristics of its dielectric medium [21].

There are two common configurations for capacitive displacement sensors that can be adapted to the intrinsic geometrical structure of a hydraulic cylinder: the flat parallel electrodes and the coaxial cylindrical electrodes configuration.

In the flat parallel electrodes configuration,  $C$  is a function of the distance between the electrodes  $d$ , the overlapping electrode surface  $A$ , and the electrical permittivity of the dielectric  $\epsilon$ :

$$C = \epsilon A / d \quad (1)$$

When applied to the hydraulic actuator, the cylinder's base and the top head surface of the piston act as electrode plates. Once a voltage is applied to the two terminals, a charge is accumulated and an electric field  $E$  builds up inside the piston chamber as shown in Fig. 2.

The disadvantage of this sensor configuration is that for values of  $d$  bigger than the sensor diameter, the electric field can no longer be considered homogeneous, and the relationship between the capacitance and the displacement is strongly nonlinear. Moreover, when miniaturizing the dimensions, the cylinder's diameter is reduced and as the electrodes' surface is proportional to  $C$  as shown in (1), the value of  $C$  would decrease. If the diameter is too small, the value of  $C$  becomes so small that it is difficult to measure.

In the case of the coaxial cylindrical electrodes configuration, the barrel and the rod act as the electrodes, see Fig. 3. When applying a voltage, the accumulation of charge on the

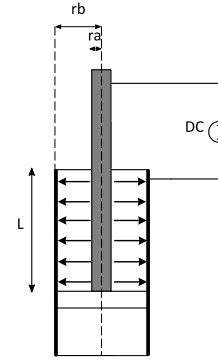


Fig. 3. Schematic of coaxial cylindrical parallel electrode configuration. The sensor's electrodes are: the barrel side and the rod, in black and grey, respectively.

plates generates a radial electric field, extending between the barrel and the rod.

In an ideal scenario, without the consideration of boundary effects, the capacitance can be calculated by (2),

$$C = \frac{2\pi \epsilon_0 \epsilon_r L}{\ln \frac{r_b}{r_a}} \quad (2)$$

where  $r_a$  denotes the radius of the inner electrode,  $r_b$  the radius of the outer electrode,  $L$  the length of the overlap of inner and outer electrodes,  $\epsilon_0$  the permittivity of free space, and  $\epsilon_r$  the relative permittivity of the dielectric between the electrodes.

The capacitance  $C$  of a coaxial cylindrical electrode sensor is proportional to the length  $L$  where the inner and the outer cylinders overlap. This principle is then used for displacement sensing.

For the deduction of formula (2) the assumption has been made that the electrode material is an ideal conductor. The electrode material can be chosen according to the medical requirements, given that this assumption remains valid.

The use of the coaxial cylindrical electrodes configuration presents several advantages in comparison to the flat electrodes configuration described earlier. From (2) it can be derived that the sensitivity of the sensor is:

$$S = \frac{2\pi \epsilon_0 \epsilon_r}{\ln \frac{r_b}{r_a}} \quad (3)$$

It is a function of the ratio between the two electrodes' radii. With the ratio getting closer to unity, the sensitivity of  $C$  increases. The sensitivity equation shows that a radial rescaling of the cylinder does not affect the sensor's sensitivity if the ratio between the outer and inner electrode diameters remains constant. This is an advantage for miniaturization. Hence, the coaxial cylindrical electrode configuration is most suitable for this hydraulic actuator displacement sensing application.

### B. FEA Simulation Results

In order to prove the validity of the concept, Ansys Maxwell FEA software was used to investigate the distribution of the electric field in the sensor and to calculate the capacitance. Three designs have been investigated. Table I contains their relevant dimensions and the voltage applied.

TABLE I  
SIMULATED MODEL DIMENSIONS AND VOLTAGE

Design	Barrel diameter (mm)	Barrel length (mm)	Rod diameter (mm)	Rod length (mm)	Voltage applied (V)
A	10	55	8	70	5
B	10	55	3	70	5
C	2.5	13.8	2	25	5

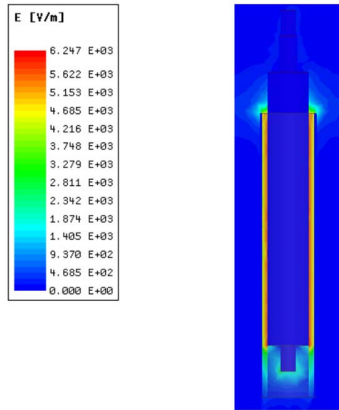


Fig. 4. Electric field distribution in the longitudinal cross-section of design A; calculated using the FEA software Ansys Maxwell.

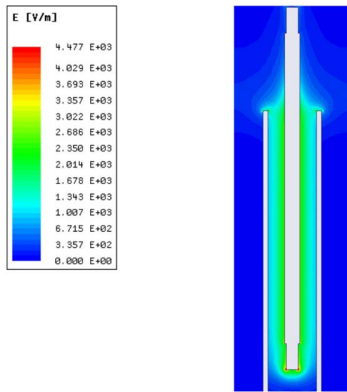


Fig. 5. Electric field distribution in the longitudinal cross-section of design B; calculated using the simulation FEA software Ansys Maxwell.

Designs A and B belong to the category of mini-hydraulic drives. Design C has the dimensions of the miniaturized hydraulic drive designed specifically for the laparoscopic instruments presented in [13].

Fig. 4 and Fig. 5 show the electric field distribution in designs A and B, respectively. The relationships between capacitance and displacement for both designs A and B are displayed in Fig. 6. They appear very linear. The slope of the capacitance against displacement graph for design B, hence the sensitivity of the sensor, is smaller than in design A. The reason is that in design A, the ratio between the external and internal electrode diameter is closer to 1 than in design B. This supports the statement that it is preferable to manufacture the rod and barrel with diameters of similar size in order to increase the sensor’s sensitivity, as predicted in II-A.

Fig. 7 shows the plot of the capacitance against displacement for the designs A and C. Fig. 8 shows the electric

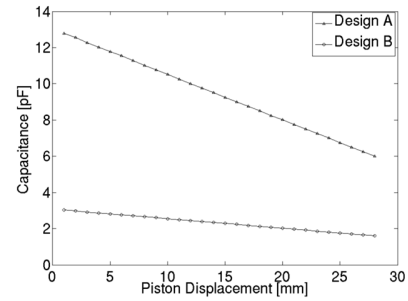


Fig. 6. Plot of capacitance against displacement for design A and B; calculated using the FEA software Ansys Maxwell.

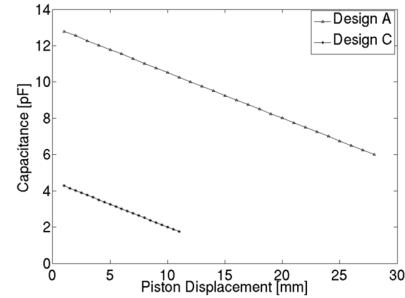


Fig. 7. Plot of capacitance against displacement for design A and C; calculated using the FEA software Ansys Maxwell.

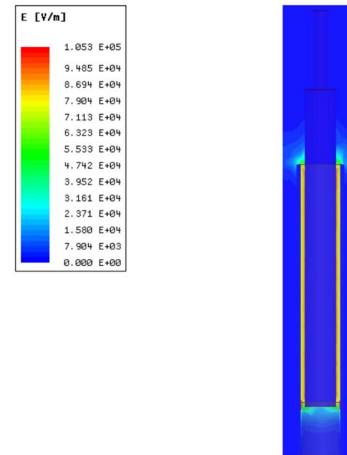


Fig. 8. Electric field distribution in the longitudinal cross-section of design C; calculated using the FEA software Ansys Maxwell.

field distribution of design C. The sensitivities of both designs are identical. However, the capacitance range in design C is smaller compared to design A, as the lengths of the rod and the barrel are significantly smaller. This proves the assertion made in section II.A, that the sensitivity of the sensor will not be affected if the piston’s dimensions are scaled, as long as the ratio of the rod and the barrel diameters remains constant.

The sensor may be affected by mechanical imperfections. An eccentric position of the rod and its misalignment with respect to the longitudinal axis of the barrel are considered to be most critical. Both imperfections are investigated in realistic scenarios.

Design A is simulated with a 0.2 mm eccentricity of the rod; the maximum mechanical manufacturing tolerance of the

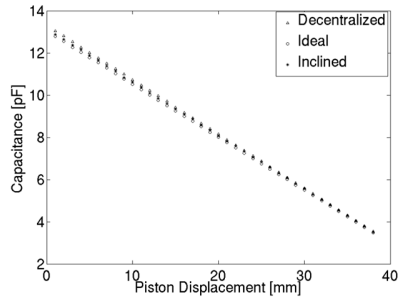


Fig. 9. Capacitance against displacement for design A, in the ideal, eccentric, and in the inclined case; calculated using the FEA software Ansys Maxwell.

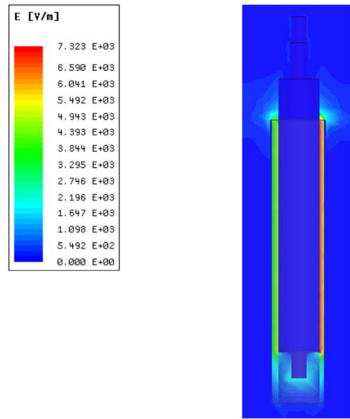


Fig. 10. Electric field distribution in the longitudinal cross-section of design A, where the rod is eccentric; calculated using the FEA software Ansys Maxwell.

cylinder prototype. To simulate the effect of the rod being inclined with respect to the longitudinal axis of the barrel, the rod is tilted by 0.2 degrees, which is the maximum manufacturing tolerance of the piston. Fig. 9 shows the capacitance against displacement plots for both cases.

In the case of the eccentric rod, the capacitance against displacement plot remains linear, but the gradient of the plot has changed compared to the ideal scenario.

With the misaligned rod, a nonlinear characteristic is expected, but a slope variation is observed, because the small tilt angle causes a negligible nonlinear effect. As expected, with the asymmetric arrangement an asymmetric electric field distribution can be observed in both cases (see Fig. 10 and Fig. 11) when compared to the ideal scenario in Fig. 4.

### III. EXPERIMENTAL ANALYSIS

#### A. Experimental Set up

In order to test the concepts described above experimentally, a test rig, shown in Fig. 12, was developed.

The rig contained a mini-hydraulic cylinder with a diameter of 10 mm and a length of 55 mm, which matched the dimensions of design A in section II-B. The two parts used as electrodes were manufactured from stainless steel and were electrically isolated from the rest of the test rig. This test rig was made adaptable in order to fit a miniaturized cylinder with the dimensions of design C in Table I (see Fig. 13).

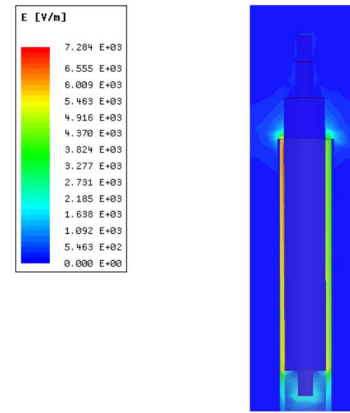


Fig. 11. Electric field distribution in the longitudinal cross-section of design A, where the rod is inclined respect to the barrel longitudinal axis; calculated using the FEA software Ansys Maxwell.

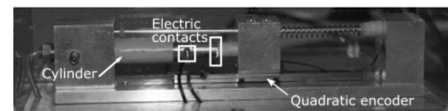


Fig. 12. Test rig used for experiments on the mini hydraulic actuator.

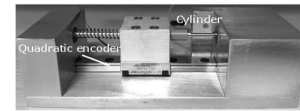


Fig. 13. Test rig adapted for a miniaturized cylinder with the dimensions of design C in Table I.

The test rigs were equipped with a Schneeberger Miniscale Plus quadratic encoder: a displacement sensor selected for its precision, reliability, and resolution of 0.1  $\mu\text{m}$ . It was used as a reference to check the position precision of the capacitive sensor system.

In order to avoid interference from the environment, the test rig was shielded.

For the capacitance measurement acquisition, a Texas Instruments FDC1004 capacitance to digital converter was used.

The cylinder's displacement was controlled using a Cetoni neMESYS syringe pump, which enabled the dosing of a defined liquid volume to the cylinder with great precision. The pump and the hydraulic actuator were connected with silicon tubes. Air was removed from the hydraulic circuit before operation. Water was used as the hydraulic medium.

#### B. Mini-Hydraulic Drive: Results

In order to evaluate the performance of the sensor, measurements were taken over a period of ten motion cycles. Every cycle consisted of extension and retraction of the syringe pump with constant step sizes. During those cycles, the capacitance of the integrated sensor and the displacement of the mini-hydraulic piston rod (via the encoder) were recorded. Four experiments were carried out with syringe volume increments which corresponded to a theoretical mini-hydraulic cylinder displacement of 1 mm, 0.5 mm, 0.05 mm, and 0.025 mm.

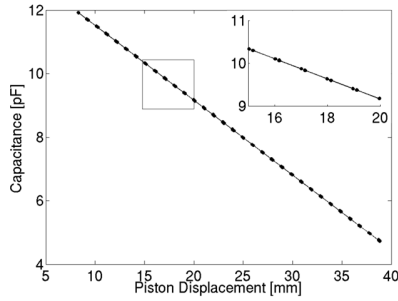


Fig. 14. Capacitance against displacement of mini-hydraulic cylinder for 1 mm position increment, taken over ten motion cycles (with detail view).

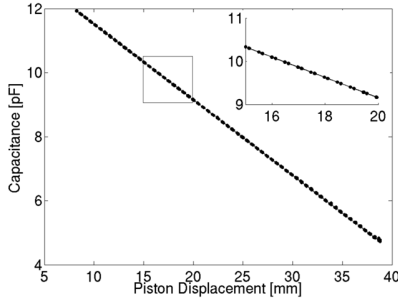


Fig. 15. Capacitance against displacement of mini-hydraulic cylinder for 0.5 mm position increment, taken over ten motion cycles (with detail view).

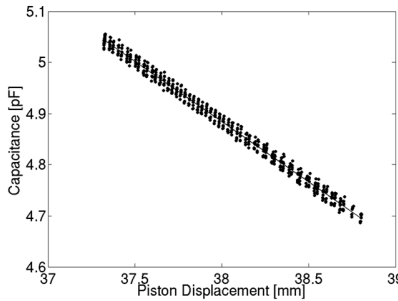


Fig. 16. Capacitance against displacement of mini-hydraulic cylinder for 0.05 mm position increment, taken over ten motion cycles.

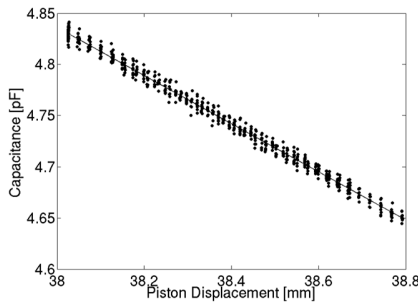


Fig. 17. Capacitance against displacement of mini-hydraulic cylinder for 0.025 mm position increment, taken over ten motion cycles.

Fig. 14 to Fig. 17 show the plot of capacitance against recorded displacement for the aforementioned motion cycles.

A least square regression analysis with a first order polynomial  $y = ax + b$  was applied to the measurements. Table II shows the results of the statistical analysis, where  $a$  and  $b$  are the coefficients of the regression model. R-squared is the

TABLE II  
RESULTS OF THE STATISTICAL ANALYSIS FOR  
MINI-HYDRAULIC ACTUATOR

Increment [mm]	$b$	$a$	R-squared	RMSE [pF]
1	13.8730	-0.2356	1.0000	0.0044
0.5	13.8685	-0.2358	1.0000	0.0076
0.05	13.8406	-0.2357	0.9922	0.0091
0.025	13.7778	-0.2353	0.9921	0.0047

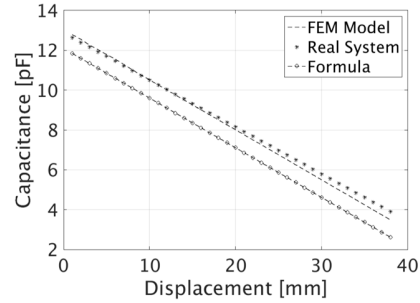


Fig. 18. Comparison between the experimental results, the FEA model and the analytic model (2) for the mini hydraulic sensor.

coefficient of determination and its value provides a measure of how well the measured data fits the statistical model. RMSE is the root mean squared error and is the measure of the average of squared difference between the measured values and the values estimated by the model.

### C. Mini-Hydraulic Drives: Discussion

The results from the experimental investigation indicate a linear sensor characteristics, which is confirmed by the least square regression analysis. The linear regression model matches the measured data with an R-squared value of 1, which shows that there is an almost perfect fit between the data and the linear model.

The sensitivity  $S$  of the sensor can be calculated as the gradient of the capacitance against displacement plot and corresponds to the parameter  $a$  of the linear regression model.

When comparing the sensor characteristics obtained from the FEA simulation with the experimental data in Fig. 18, a close correspondence between the results is observed. The difference between the gradients can be explained by mechanical imperfections resulting from the manufacturing process. Both plots show higher values than those predicted by (2), because boundary effects of the electric field and material characteristics of the electrodes are neglected in this equation.

The precision can be deduced from the RMSE. By using the average of the RMSE in all the measurements taken and multiplying it with the gradient of the capacitance-displacement plot, it is possible to conclude that the system is able to measure with an average precision of  $\pm 27 \mu\text{m}$ .

Additionally, it is observed that the initial and final position of the piston were never exactly matching, indicating the presence of mechanical hysteresis. In order to examine this in detail, the quadratic encoder was used. The measurement of the piston displacement against the liquid volume in the syringe pump, hence in the cylinder, was recorded. It is

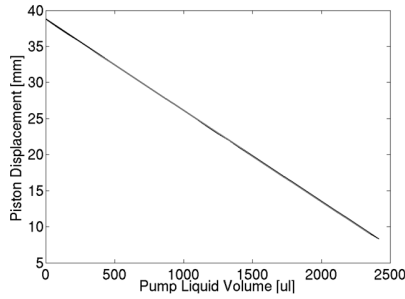


Fig. 19. Mini-hydraulic cylinder displacement against syringe pump volume.

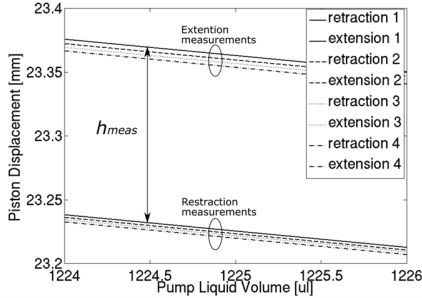


Fig. 20. Magnified view of Fig. 19 for consecutive extension and retraction movements.

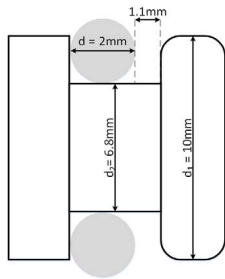


Fig. 21. Cross-section of the cylinder piston to show the piston design and ring sealing dimensions.

plotted in Fig. 19 and Fig. 20, where the latter is a zoomed view. The plots are concentrated into two groups: retraction and extension. The difference in displacement between extension and retraction is the same in every cycle and its measure  $h_{meas} = 0.132$  mm. Additionally, there is a constant shift downwards to a lesser displacement with every measurement cycle. This continuous reduction in displacement for every cycle can be explained by small amounts of leakage out of the system. The reason for the difference between the extension and retraction movement per cycle is the mechanical construction of the piston seal and its mechanical play.

In order to understand the hysteresis effect, Fig. 21 shows a cross-section of the piston, together with the piston and O-ring seal dimensions. It can be seen that the slot for the seal is wider than the seal itself. This means that when extending the piston, the seal is pushed towards the right side of this slot, whereas when retracting, it is pulled towards the left. Therefore, the volume of the piston chamber is larger during retraction than during extension. When retracting, some of the liquid volume flows in the seal slot without moving the piston. In order to prove this hypothesis, the volume of liquid corresponding to

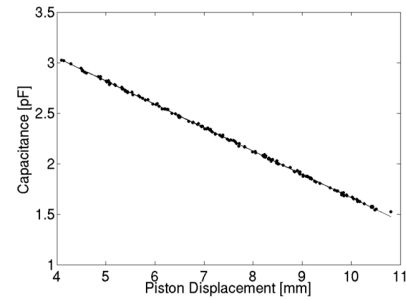


Fig. 22. Capacitance against displacement plot for the micro-hydraulic actuator at 200 random positions.

TABLE III  
RESULTS OF THE STATISTICAL ANALYSIS FOR THE  
MINIATURIZED HYDRAULIC ACTUATOR

$b$	$a$	R-squared	RMSE (pF)
3.9738	0.2311	0.9995	0.0091

the seal movement has been calculated and compared to the measured offset.

The volume available in the seal slot is:

$$V_{gap} = \pi h \left[ \left( \frac{d_1}{2} \right)^2 - \left( \frac{d_2}{2} \right)^2 \right] \quad (4)$$

This volume can cause an offset in piston displacement of  $h_{theo} = 0.591$  mm.

The theoretical value has the same order of magnitude as the measured offset, but it is approximately 4.5 times larger. The difference can be explained by the fact that the free volume in the seal slot is smaller than the theoretically expected value, because some of it is filled with lubrication grease.

The hysteresis can already be observed in the plot in Fig. 14 and Fig. 15, in which the measurements recorded per step are concentrated into two clouds of points which almost overlap.

All measurements were executed with the setup shielded, in order to reduce external interferences on the measurements. For a final sensor-actuator design, a solution for the integration of both the sensor and the shield into the laparoscopic instrument must be found. This will require a conductive material cover surrounding the hydraulic drive and an electric isolation between the rod and the instrument tip.

#### D. Miniaturized Hydraulic Drive: Results and Discussion

To prove the simulation results for the miniaturized-hydraulic drives the test rig shown in Fig. 13 was used.

The performance of the sensor was evaluated with 200 measurements, taken with random movements of the piston. Fig. 22 shows the result of the measurements.

The miniaturized version of the sensor demonstrated a similar linear behavior to the mini-hydraulic drive, confirmed by the least square regression analysis. Table III shows the statistical analysis parameters for the fit.

Like the experimental results of the mini-hydraulic drive, in this experiment, R-squared is approximately 1, which indicates that the fit between the data and the linear model is good.

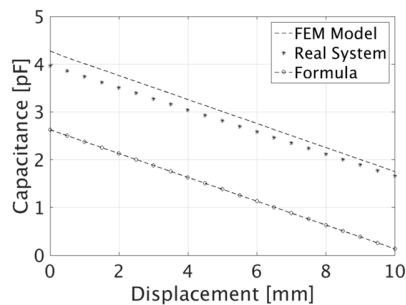


Fig. 23. Comparison between the experimental result, the FEA model and the simplified formula (2) for the miniaturized hydraulic sensor.

Fig. 23 demonstrates the good correspondence between the results of the FEA simulation and the experimental results. The two plots have a different slope which is explained by the mechanical imperfection caused by the manufacturing tolerances. Both plots show greater values than those predicted by (2). This would be expected, as in the equation both boundary effects of the electric field and material characteristics are neglected.

The sensor has a precision of  $\pm 38 \mu\text{m}$ . As with the mini-hydraulic drives, the sensor has been shielded during all the experiments.

#### IV. CONCLUSIONS

The design principle of a position sensor integrated into a miniaturized-hydraulic actuator was investigated. The feasibility of a coaxial cylindrical capacitive sensor was theoretically analyzed and validated with a FEA simulation and an analytic model. It was shown that a radial rescaling of the cylinder did not affect the sensor's sensitivity. Also, it was shown, that mechanical imperfections due to manufacturing tolerances did not severely influence the sensor's linear characteristics.

An experimental setup was developed for a mini-hydraulic drive and a miniaturized-hydraulic drive to validate the analytical and simulation results. The experimental results matched the simulations and confirmed the linearity of the relationship between the capacitance and displacement for both sensorized drives with a precision of  $\pm 27 \mu\text{m}$  for the mini-hydraulic actuator and  $\pm 38 \mu\text{m}$  for the miniaturized hydraulic actuator.

The sensor-actuator design was shown to have the potential to be integrated into laparoscopic instruments to improve their positioning precision. However, since the measurements were taken with an electrically shielded sensor, such shielding would have to be incorporated in the final design.

The shield integration will be the subject of future research in addition to further investigations into the design of the hydraulic control circuit.

#### ACKNOWLEDGMENTS

The authors would like to thank Nikolaos Deliolanis for critically reading and commenting the manuscript.

#### REFERENCES

[1] R. Autorino *et al.*, "Current status and future perspectives in laparoscopic single-site and natural orifice transluminal endoscopic urological surgery," *Int J. Urol.*, vol. 17, no. 5, pp. 410–431, 2010.

[2] G.-P. Haber *et al.*, "Robotic notes (natural orifice transluminal endoscopic surgery) in reconstructive urology: Initial laboratory experience," *Urology*, vol. 71, no. 6, pp. 996–1000, 2008.

[3] A. Rané, G. Y. Tan, and A. K. Tewari, "Laparo-endoscopic single-site surgery in urology: Is robotics the missing link?" *BJU Int.*, vol. 104, no. 8, pp. 1041–1043, 2009.

[4] R. Miniati *et al.*, "Hospital based economic assessment of robotic surgery," in *Proc. Medit. Conf. Med. Biol. Eng. Comput. (IFMBE)*, 2014, pp. 1144–1146.

[5] T. Bensignor, G. Morel, D. Reversat, D. Fuks, and B. Gayet, "Evaluation of the effect of a laparoscopic robotized needle holder on ergonomics and skills," *Surg Endosc.*, vol. 30, no. 2, pp. 446–454, 2016.

[6] M. Zdichavsky, M. Krautwald, M. V. Feilitzsch, D. Wichmann, A. Königsrainer, and M. O. Schurr, "Laparoscopic gastro-jejunal anastomosis using novel r2 deflectable instruments in an *ex vivo* model," *Minimally Invasive Therapy Allied Technol.*, vol. 25, no. 2, pp. 91–98, 2015.

[7] M. de Volder, "Pneumatic and hydraulic microactuators: A new approach for achieving high force and power densities at microscale," Katholieke Univ. Leuven, Leuven, Tech. Rep. UDC 621-181.48, 2007. [Online]. Available: <https://lirias.kuleuven.be/handle/1979/834>

[8] M. D. Volder and D. Reynaerts, "Pneumatic and hydraulic microactuators: A review," *J. Micromech. Microeng.*, vol. 20, no. 4, p. 43001, 2010. [Online]. Available: <http://stacks.iop.org/0960-1317/20/i=4/a=043001>

[9] T. Cuntz, G. James, V. Valkov, A. Sanagoo, and D. Kaltenbacher, "Next generation surgical instruments powered by hydraulics," *Biomed. Eng./Biomedizinische Techn.*, vol. 58, no. suppl 1, Aug. 2013.

[10] T. Cuntz and L. Comella, "Design and control of a 3-DOF hydraulic driven surgical instrument," *Current Directions Biomed. Eng.*, vol. 1, no. 1, pp. 140–144, Sep. 2015.

[11] M. Lazeroms *et al.*, "A hydraulic forceps with force-feedback for use in minimally invasive surgery," *Mechatronics*, vol. 6, no. 4, pp. 437–446, 1996.

[12] C. Spindler, D. Kaltenbacher, and J. Schähte, "Powerful microactuators for (flexible) surgical instrument tips," in *Proc. Biomed. Techn.*, 2013, pp. 1–2.

[13] T. Cuntz, *Untersuchungen zur Eignung Mikrohydraulischer Antriebe für die Minimal Invasive Chirurgie*. Stuttgart, Germany: Fraunhofer Verlag, 2016.

[14] I. L. Krivts and G. V. Krejnin, *Pneumatic Actuating Systems for Automatic Equipment: Structure and Design*. Boca Raton, FL, USA: CRC Press, 2006.

[15] B. Hodges, "Position sensors for hydraulic cylinders," in *Proc. Int. Off-Highway Powerplant Congr. Expo., SAE Int. 400 Commonwealth Drive*. SAE international, Warrendale, PA, USA, 1993.

[16] H. Zhu and W. J. Book, "Construction and control of massive hydraulic miniature-actuator-sensor array," in *Proc. IEEE Conf. Comput. Aided Control Syst. Design, IEEE Int. Conf. Control Appl. IEEE Int. Symp. Intell. Control*, Oct. 2006, pp. 820–825.

[17] M. De Volder, J. Coosemans, R. Puers, and D. Reynaerts, "Characterization and control of a pneumatic microactuator with an integrated inductive position sensor," *Sens. Actuators A, Phys.*, vol. 141, no. 1, pp. 192–200, 2008.

[18] H. Sumali, E. P. Bystrom, and G. W. Krutz, "A displacement sensor for nonmetallic hydraulic cylinders," *IEEE Sensors J.*, vol. 3, no. 6, pp. 818–826, Dec. 2003.

[19] E. Terzic, J. Terzic, R. Nagarajah, and M. Alamgir, "Capacitive sensing technology," in *A Neural Network Approach to Fluid Quantity Measurement in Dynamic Environments* E. Terzic, J. Terzic, R. Nagarajah, M. Alamgir, Eds. London, U.K.: Springer, 2012, pp. 11–37.

[20] J. Fraden, "Handbook of modern sensors," *Physics, Designs, and Applications*. New York, NY, USA: Springer, 2016.

[21] A. Keith, "Displacement measurement, linear and angular," in *The Measurement, Instrumentation and Sensors Handbook*. Boca Raton, FL, USA: CRC Press, 1999.

**Laura M. Comella** received the master's degree in electronic engineering from the University degli Studi di Palermo, Italy, in 2011. Since 2012, she has been a Researcher with the Project Group for Automation in Medicine and Biotechnology, Fraunhofer Institute for Manufacturing Engineering and Automation IPA, Mannheim, Germany.

**Krasimir Ayzov** is currently pursuing the master's degree in electrical and electronic engineering with the University of Bath, U.K. As part of his course, he has been doing a yearlong industrial placement with the Fraunhofer Institute for Product Automatization in Medicine and Biotechnology, Mannheim, Germany.

**Timo Cuntz** received the Dipl.Ing. degree in mechanical engineering from the Karlsruhe Institute of Technology in 2007. He was a Research Assistant with the Institute MIMED, TU Munich. In 2008, he joined the Fraunhofer Institute for Manufacturing Engineering and Automation IPA. From 2008 to 2011, he was with the Department for Production and Process Automation, Stuttgart, Germany. In 2011, he was with the newly founded Project Group for Automation in Medicine and Biotechnology in Mannheim, Germany, where he was a Research Assistant with the Research Group for Micro Mechatronic Design. Since 2014, he has been the Leader of the Research Group for Medical Assistant Systems. His focus is on micro hydraulic actuator systems for surgical instruments and medical robots.

**Auguste van Poelgeest** was born in The Netherlands in 1983. She received the M.Eng. (Hons.) degree in mechanical engineering and French from the University of Bath, Bath, U.K., in 2005, and the Ph.D. degree in mechanical engineering from the Centre for Power Transmission and Motion Control, University of Bath.

In 2011, she joined the Project Group for Automation in Medicine and Biotechnology as a Research Scientist with the Micromechatronics Team. In 2014, she started her own Research Team focusing on control systems for medical engineering. Her research interests include medical robotics, artificial intelligence for automation in medicine, and implantable devices for diagnostics and therapy.

**Jonathan Schächtele** received the Dipl.Ing. (With Distinction) degree in mechatronics from the Friedrich-Alexander Universität Erlangen-Nürnberg in 2009.

Since 2009, he has been a Research Assistant with the Fraunhofer Institute for Manufacturing Engineering and Automation (IPA). From 2009 to 2012, he was with the Department for Production and Process Automation, Stuttgart, Germany. In 2012, he was with the newly founded Project Group for Automation in Medicine and Biotechnology, Mannheim, Germany, where he is currently a Senior Scientist with the Research Group Control Systems in Medical Engineering. His focus is on micro sensor and actuator systems for active implantable devices.

**Jan Stallkamp** received the Diploma degree in aeronautical engineering from the Rheinisch-Westfälischen-Technischen Hochschule, Aachen, in 1995, and the Ph.D. degree from the University of Stuttgart in 2005, with a thesis on "Optical 3-D Measurement Device for Navigation in Robot-Assisted Keyhole Surgery." He was a Research Assistant with the Virtual Reality Group, Fraunhofer-Institute for Manufacturing Engineering and Automation IPA, Stuttgart, Germany. In 1998, he became the Head of the Competence Center for Medical Technologies, that centers the competences at the Fraunhofer IPA from the different departments. Since 2001, he was the Head of the Group Geräte-und Anlagenentwicklung, which specialized in the development of systems for life-science applications and food industry. In 2005, he was the Head of the Department for Production and Process Automation at the IPA, which has a main focus in the field of technologies for diagnosis and intervention, life-sciences, and food technology. Since 2012, he has been the Head of the Fraunhofer-Project Group for Automation in Medicine and Biotechnology at the Medical Faculty, University Heidelberg, Mannheim. In 2014, he received the professorship for Automation in Medicine and Biotechnology at the University of Heidelberg.